Observations of Martian Tides Over Two Annual Cycles[1]

CONWAY B. LEOVY

Department of Atmospheric Sciences, University of Washington, Seattle 98195

(Manuscript received 29 July 1980, in final form 16 September 1980)

ABSTRACT

The first four diurnal surface pressure harmonics have been analyzed over major portions of two Martian annual cycles (Mars years) at the two Viking lander sites. The diurnal harmonics of surface wind have also been analyzed at one of the sites. Since the atmospheric tides have previously been shown to provide a good indication of Martian global dust storms, these results provide a basis for comparing dust storm activity in the two years. Two global dust storms occurred during the first year. During the second year, there was only one major storm, and it closely followed the pattern of the first storm of the first year. A significant feature of the results is the brief, but nearly complete, vanishing of the diurnal pressure tide at the onset of one of the global dust storms. It is proposed that this may have been due to interference between the normal westward-propagating diurnal tide and a topographically forced eastward propagating tide, and that the latter may have helped initiate the global storm.

1. Introduction

The relationship between the dust content of the Martian atmosphere and thermally forced atmospheric tides has been demonstrated in several theoretical and observational studies (Zurek, 1976, 1978; Hess *et al.*, 1977; Leovy and Zurek, 1979; the latter is referred to as LZ hereafter). By absorbing solar radiation, the dust can provide a powerful thermal drive for the tides as well as for other components of the global circulation. Occasional global dust storms occur during which the opacity increases to very large values over the entire planet. In LZ, amplitudes of both diurnal and semidiurnal pressure oscillations at two Viking lander sites were shown to correlate well with local and global opacity due to dust. The semidiurnal surface wind oscillation was also closely related to atmospheric dust load.

In this study, a more detailed analysis of tidal pressure and wind variations during the first Martian year of measurements at the Viking lander sites[2] is presented, and the analysis is extended to corresponding periods of the second Martian year. The first-year analysis gives a more uniform coverage and higher time resolution than that presented in LZ, and the terdiurnal and quadridiurnal harmonics are included. These results provide the basis for the theoretical work of Zurek (1981). Since the tides provide an excellent indication of the level of global dust storm activity, the second-year analysis provides a basis for comparing the dust storm behavior in the two years (see Ryan and Sharman, 1981).

2. Tidal pressure variations

a. Analysis

Individual wind and pressure measurements for the periods analyzed were blocked into 24 equal time bins per sol. Empty bins were filled by a cubic spline fit, and any bins containing obviously erroneous data points on the basis of either the bin mean value or its variance were rejected and treated as empty. Less than 10% of the bins were empty during the first year, but about half the bins were empty for Lander 2 during the second year. Although the number of data points per bin varied, typical values were 100 for wind and 5 for pressure. Bin average values were normally composited into 10 sol groups to remove the effect of longer period variations and improve reliability of the harmonics, but data returned from Lander 1 later than sol 791 were so sparse that only a few composites, mostly of duration less than 10 sols each, could be formed. Composites of 30 sol duration were formed for summer at Lander 2 because of the low tidal amplitudes. Table 1 lists the composites.

Harmonic analysis was applied to the composited data for components 0–5, however, the fifth har-

[1] Contribution No. 548, Department of Atmospheric Sciences, University of Washington, Seattle.

[2] Viking Lander 1 is at 22.5°N latitude, 48°W longitude and Viking Lander 2 is at 48°N, 226°W. A Martian year is 669 sols; a sol, or Martian solar day, is 88 775 seconds. The Martian seasonal index is the longitude of the sun in Mars centered coordinates (areocentric longitude), L_s, measured from 0° at northern vernal equinox.

0022-4928/81/010030-10$06.50
© 1981 American Meteorological Society

Unauthenticated | Downloaded 03/03/24 03:50 PM UTC

TABLE 1. Harmonic analyses by sol number. Entry 141(5)176 indicates composite centered on Lander 1, sol 141 and at 5 sol intervals to Lander 1, sol 176. Column labeled length (sols) is the number of sols in each composite. Lander 1, sol number 1 was at L_s = 97°; Lander 2, sol number 1 was 45 sols later at L_s = 117°.

	Lander 1			Lander 2		
	Lander 1 Sol number	Areocentric longitudes (L_s)	Length (sols)	Lander 2 Sol number	Areocentric longitudes (L_s)	Length (sols)
Year one	55	122	10	46	140	30
	141(5)176	167–187	10	150(5)330	198–312	10
	190(5)320	195–279	10	336(5)436	316–010	10
	329(5)369	284–309	10			
	379(5)389	315–321	10			
	397(5)477	325–008	10			
Year two	756(5)791	138–157	10	715	140	30
	853	192	3	811(5)851	193–218	10
	918	232	10	860	224	10
	970	266	2	875	233	10
	1014	294	13	878(5)948	235–281	10
	1071	328	7	970(5)995	294–310	10
	1131	001	8			

monic was small and inconsistent and results are not presented here.

b. Results

The surface pressure amplitude ratio $\delta p/\bar{p}$ for the diurnal and semidiurnal tides are shown in Figs. 1 and 2. The global dust storms of the first year are marked by sharp rises in both tidal amplitudes near L_s = 200 and L_s = 270, especially well shown by the semidiurnal tide at Lander 1. These tidal events, which are referred to below as 1977a and 1977b, have been described in detail in LZ. Other features of the associated global dust storms can be found in Briggs *et al.* (1979), Martin and Kieffer (1979), Ryan and Henry (1979) and Pollack *et al.* (1979). The striking regular double-sawtooth behavior of the Lander 1 semidiurnal tide is due to its very close

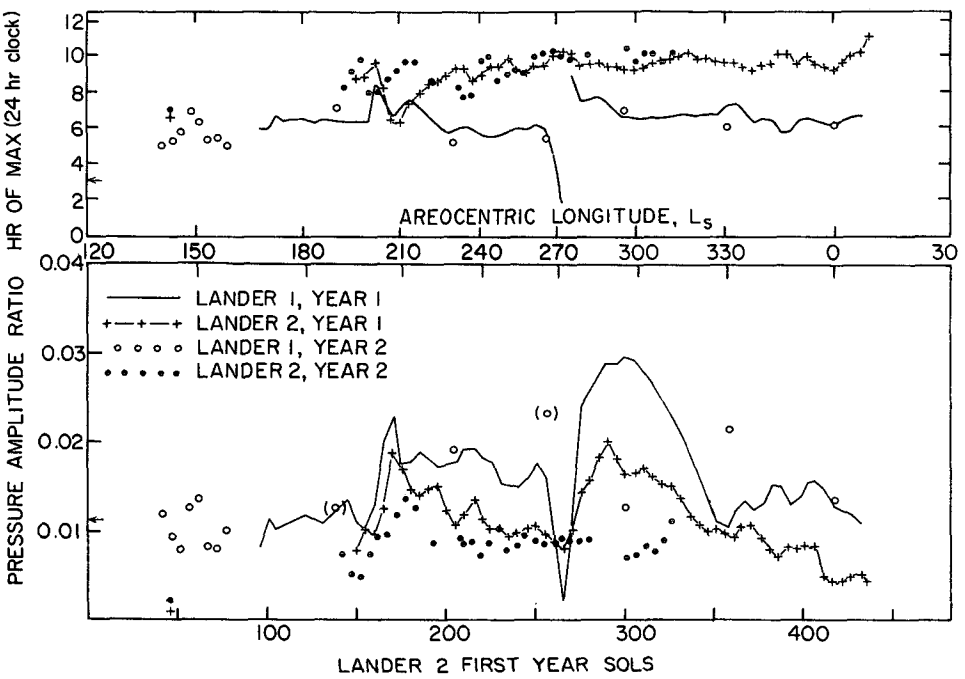

FIG. 1. Amplitude (lower) and phase (upper) of the Martian diurnal tide at two sites during two years. Amplitudes are for the pressure ratio, $\delta p/\bar{p}$. Arrow at the left-hand margin indicates the amplitude at first year sol 55. The second year Lander 1 values in parentheses are less reliably determined.

Unauthenticated | Downloaded 03/03/24 03:50 PM UTC

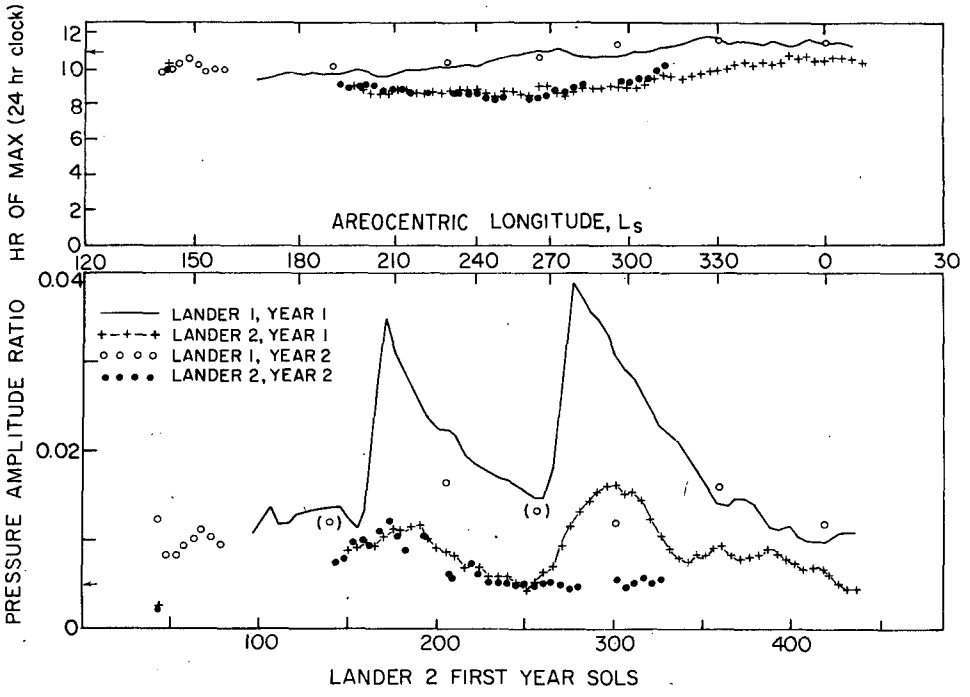

FIG. 2. Same as Fig. 1 for the semidiurnal tide.

connection to the dust opacity which varied in the same way (Zurek, 1981).

Comparing years, note that the Lander 2 tides follow an almost identical pattern during the period from $L_s = 180$ to $L_s = 260$. In particular, the Lander 2 data indicate an event occurring at the same season as 1977a with the same duration and the same semidiurnal amplitude but with a somewhat smaller diurnal amplitude. This event will be referred to as 1979a. Lander 1 data are too sparse to define this event well, but the semidiurnal amplitude observed at $L_s = 230$ suggests that it was distinctly less intense than 1977a. During the period up to $L_s = 313$ there was no event corresponding to 1977b, as shown by the Lander 2 tides and the Lander 1 data point at $L_s = 297$ of the second year. The large Lander 1 diurnal amplitude at second-year $L_s = 266$ is unreliable because of the small amount of data in that composite (Table 1). There may have been a small second-year tidal amplification at Lander 1 between $L_s = 297$ and $L_s = 331$, but the semidiurnal tide at $L_s = 331$, which is well determined by the data, shows that it could not have been comparable to 1977b in intensity.

A significant feature in Fig. 1 is the amplitude loss of the diurnal tide at Lander 1 at the onset of 1977b. This amplitude dropout was not identified in LZ because of large gaps in the tidal sampling in that study. Rapid shifts in diurnal tidal phase occur on both sides of this dropout. Composites at the time of the dropout, 20 sols earlier and 19 sols later, clearly show the sharp decrease and subsequent even sharper rise in the diurnal harmonic (Fig. 3).

Tidal phases in the two years track each other very closely, show significant phase shifts with

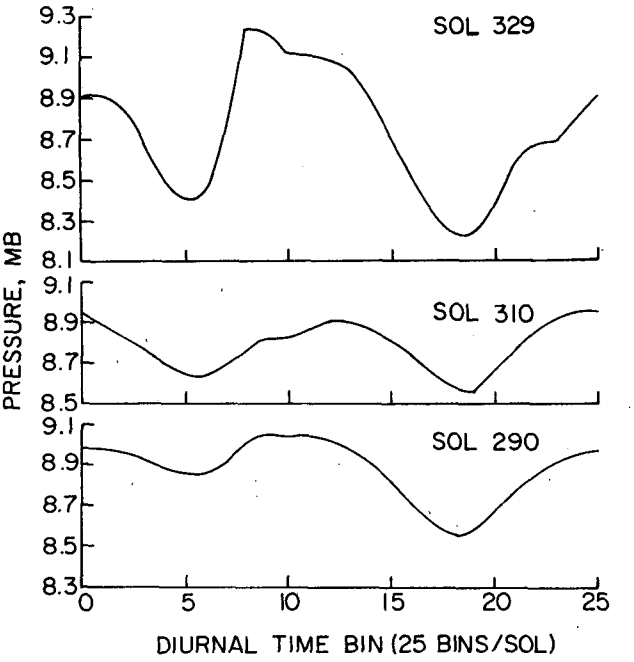

FIG. 3. Composite Lander 1 diurnal pressure curves centered on Lander 1 sols 290, 310 and 329. Note that these curves are based on composites of 25 bins per sol.

Unauthenticated | Downloaded 03/03/24 03:50 PM UTC

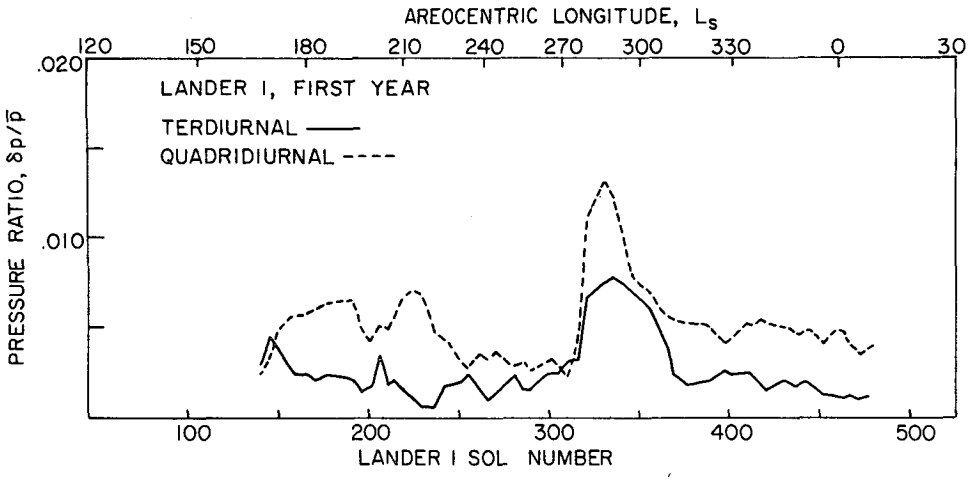

FIG. 4. Amplitudes of the terdiurnal and quadridiurnal pressure ratios ($\delta p/\bar{p}$) at Lander 1 during the first year.

latitude (diurnal phase lag and semidiurnal phase advance with latitude), and except for the period around the Lander 1 diurnal tidal dropout, they show little or no influence of the global dust storm events. There is a general tendency for phase retardation as the season advances toward spring, especially in the semidiurnal tide.

Fig. 4 shows the terdiurnal and quadridiurnal tides at Lander 1 during the first year. The sharp peak corresponding to 1977b appears in both components, but there is little or no indication of the 1977a event. Zurek's calculations show these features for the terdiurnal tide,[3] but they do not show such a strong 1977b response for the quadridiurnal tide. Terdiurnal and quadridiurnal tidal amplitudes were small throughout the second year, further indicating the absence of a feature comparable to 1977b. Terdiurnal and quadridiurnal phases, show a general tendency for phase retardation with season (Fig. 5).

[3] The author communicated most of the results presented here to Zurek during the course of the latter's analysis, without including the terdiurnal tide, but with the comment that it was generally not significant. Thus, in an early draft of his paper, Zurek indicated that the terdiurnal jump during 1977b was at variance with the data. It was only after receiving a copy of Zurek's draft that the terdiurnal jump shown in Fig. 4 was noticed in the data.

3. Tidal winds

a. Wind hodographs

Lander winds were binned, composited, and harmonically analyzed as described in the preceding section. Because of a Lander 1 instrument failure, only Lander 2 winds were used. In Fig. 6, 10 sol diurnal wind hodographs at comparable times during the two years are compared. Panels (a) and (b), for midsummer, show almost identical hodographs, except for a slight shift in mean wind (magnitude $\lesssim 0.4$ m s^{-1}). Since interdiurnal variability is nearly absent, and atmospheric dust load is low, year-to-

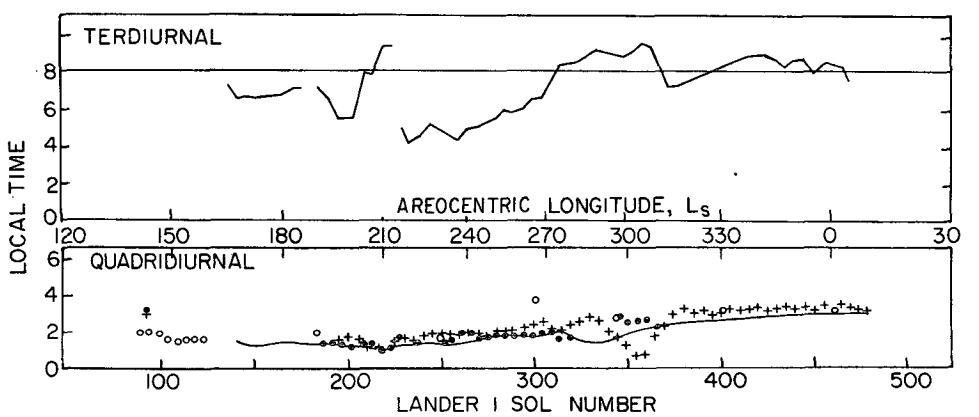

FIG. 5. Phases of the terdiurnal and quadridiurnal tides.

Unauthenticated | Downloaded 03/03/24 03:50 PM UTC

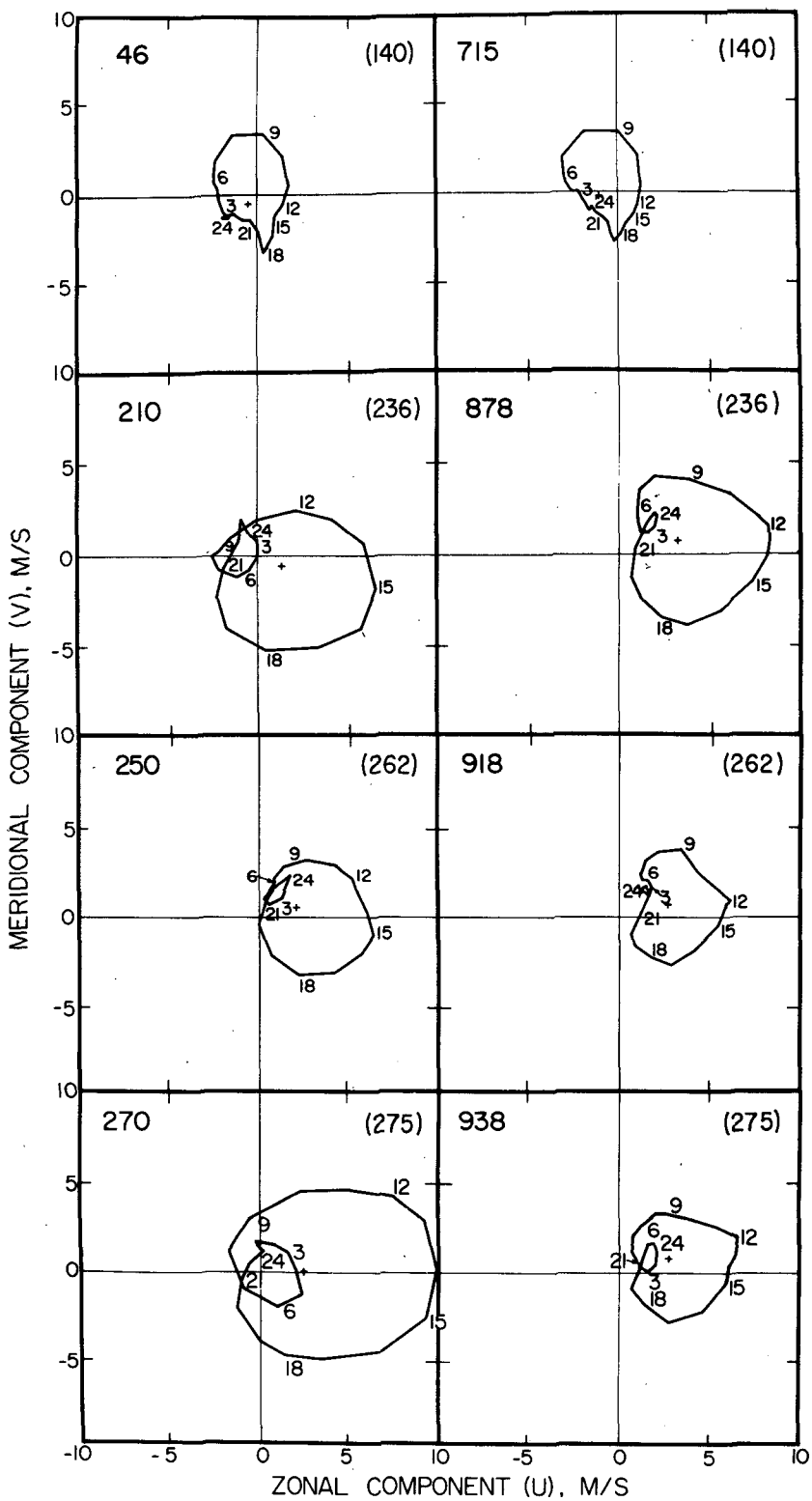

FIG. 6. Diurnal wind hodographs at Lander 2. Numbers indicate Martian local times (24 h clock). Crosses indicate daily mean wind. Lander 2 sol numbers are shown along with L_s values (in parentheses).

Unauthenticated | Downloaded 03/03/24 03:50 PM UTC

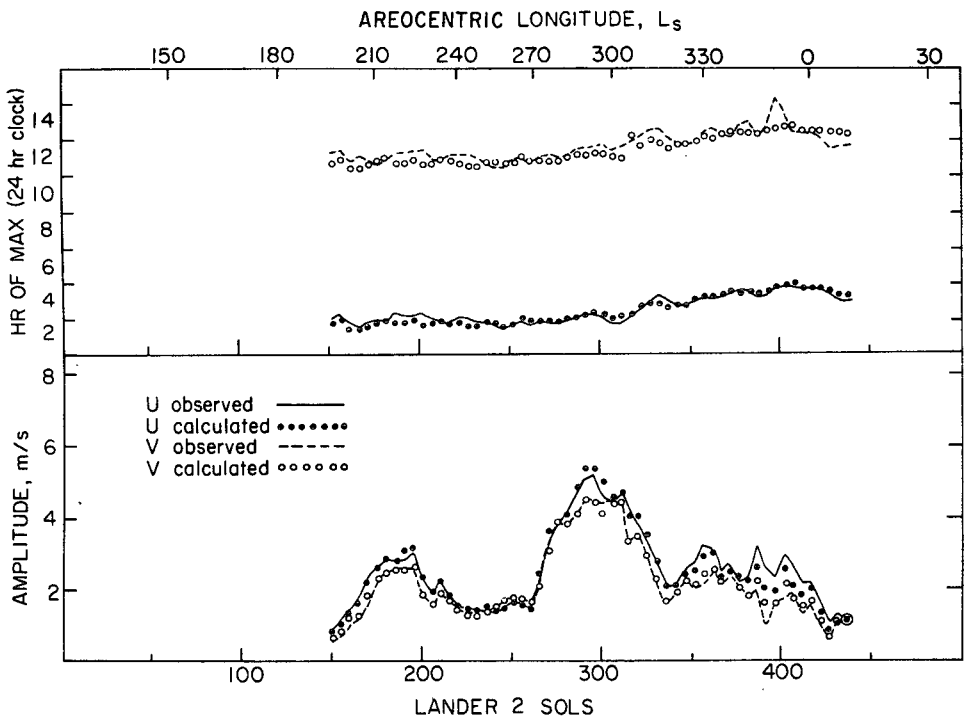

FIG. 7. Comparison of observed and calculated eastward (u) and northward (v) semidiurnal winds, Lander 2, first year. Calculations were made using the Ekman-layer model described in the text.

year wind variations are likely to be minimal at this season. Thus, this comparison gives an indication of the long-term repeatability of the wind measurement system when data are composited in this way. The remaining hodograph pairs are also generally similar except for the period later than $L_s = 270$, when weak second-year winds also indicate that the 1977b event did not repeat in 1979.

b. *Semidiurnal wind model*

In LZ, the semidiurnal wind variation was related to the semidiurnal pressure variation by means of a simple, rotating Ekman-layer model, under the assumption that the semidiurnal tide is a global-scale westward-propagating mode of zonal wavenumber $s = 2$. This procedure fails for the diurnal tide because the diurnal wind is strongly influenced by regional and local pressure gradients and by the diurnal variation in stability (Hess *et al.*, 1977). Stability variations also affect the semidiurnal winds, causing a much smaller hodograph loop during the night than during the day (Fig. 6), but they do not strongly affect the wind component phase relationships. Consequently, this oversimplified model worked well and convincingly demonstrated that the semidiurnal pressure oscillation was indeed due to a westward-traveling global $s = 2$ mode.

The model yielded predicted surface winds at lander measurement height z_m (1.61 m) in terms of the diurnal pressure variation and a free parameter, $\beta \equiv (Kf/2\omega_0^2)^{1/2}$, where K is a constant eddy viscosity coefficient, f the Coriolis parameter, and ω_0 a surface layer frictional coefficient (see the Appendix).

In this study, the model was applied to the Lander 2 pressure-wind composites for both years, allowing two free parameters: β and also γ, the ratio of the meridional pressure gradient, $\Lambda \equiv -\partial(\delta p/\bar{p})/\partial\phi$, to the amplitude of the pressure oscillation $|\delta p/\bar{p}|$. This quantity is complex because the phase of Λ may differ from the phase of $\delta p/\bar{p}$, but tests showed that the best overall agreement occurred for zero phase difference, so that γ was taken to be real. It was also constrained to lie between 0.75 and 3.25. For each composite, the values of β and γ were found which minimized the squared residuals between the sine and cosine coefficients of the observed and model eastward and northward components of the semidiurnal wind. Thus four quantities were determined from a model with two free parameters.

Amplitudes and phases of the observed winds are compared with the model in Figs. 7 and 8. Agreement is excellent during the first year, but is less satisfactory during the second year as a consequence of a phase advance of the observed wind

Unauthenticated | Downloaded 03/03/24 03:50 PM UTC

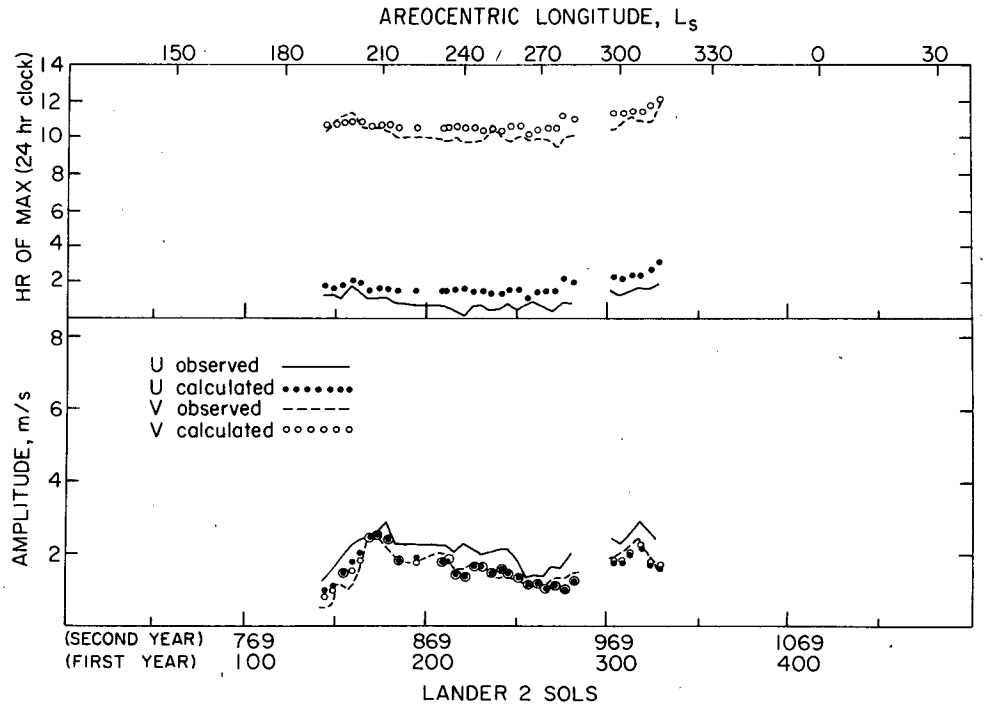

FIG. 8. As in Fig. 7 except for the second Mars year.

components relative to pressure. It was found that a uniform phase advance of γ did not materially improve the agreement during the second year. The reason for this phase shift in semidiurnal winds is unknown.

If it is assumed that ω_0 is independent of frequency, the ratio of wind speed at z_m to the inviscid wind speed at zero frequency can be derived from the values of β. This ratio is the square root of geostrophic drag coefficient $C_g^{1/2}$ evaluated at z_m; the analysis also yields the cross-isobar inflow angle at z_m (see the Appendix). Deduced values of $C_g^{1/2}$ are shown in Fig. 9. These fall in the range of 0.3 to 0.6 with the higher values tending to occur during the global dust storms of the first year when winds were strongest.

The model is not very sensitive to values of γ within the range 0.75 to 3.25. In most cases, the contours of model residual plotted in the $\beta-\gamma$ plane had a long trough running roughly parallel to the γ axis. Thus γ is not well determined by the model; nevertheless, deduced values generally were sensible. This is indicated in Fig. 10 in which smoothed values of γ from the model are compared with the uncentered finite difference approximation $2\Delta\phi^{-1}[|\delta p/\bar{p}|_i - |\delta p/\bar{p}|_2] \approx [|\delta p/\bar{p}|_1 + |\delta p/\bar{p}|_2]^{-1}$, where $|\delta p/\bar{p}|_i$ is the pressure amplitude ratio at site i, and $\Delta\phi$ is the latitude separation.[4] If only the dominant semidiurnal mode ($S_2^{2,2}$) were contributing, the value of γ at the Lander 2 site would be $\sim$5.0, and the value of the finite difference approximation would be 2.8; for the Earth, the corresponding values are about 2.6 and 1.9 (Chapman and Lindzen, 1970). The Martian semidiurnal tide appears to have a meridional structure like that of the Earth's tide. Since the landers are nearly 180° apart in longitude, the good correspondence be-

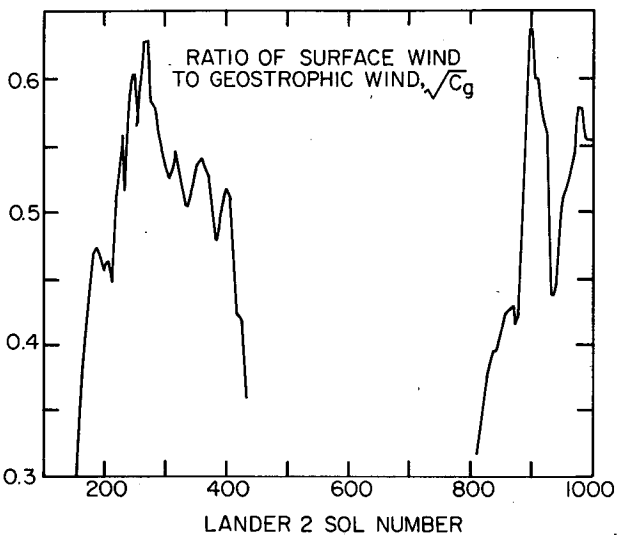

FIG. 9. Square root of the geostrophic drag coefficient ($C_g^{1/2}$) deduced from the Ekman layer model.

[4] Note that only magnitudes of the pressure ratios appear because phases of the pressure variations are assumed to have no latitude dependence.

Unauthenticated | Downloaded 03/03/24 03:50 PM UTC

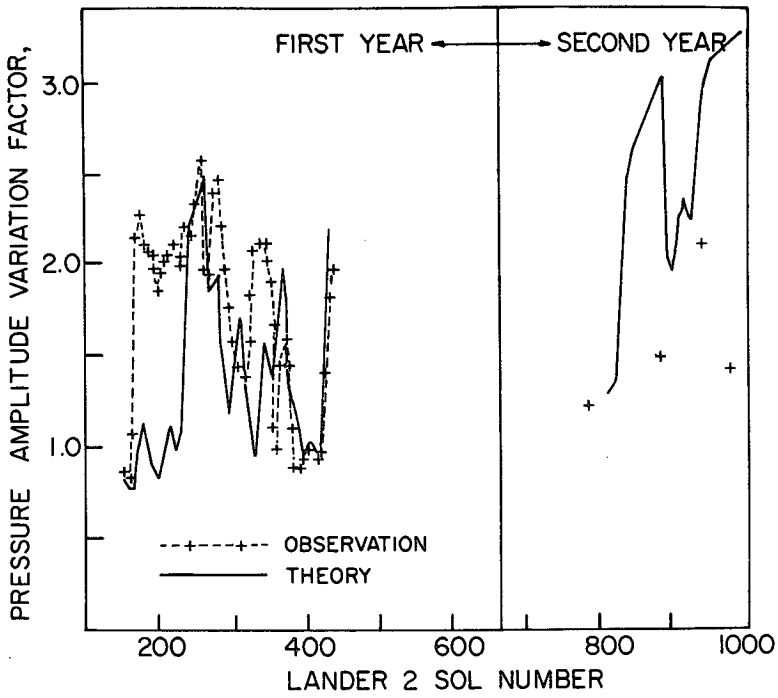

FIG. 10. Comparison between the parameter γ measuring meridional pressure gradient deduced from the model (theory) with the uncentered finite-difference approximation $2\Delta\phi^{-1}[|\delta p/\bar{p}|_1 - |\delta p/\bar{p}|_2] \div [|\delta p/\bar{p}|_1 + |\delta p/\bar{p}|_2]$ (observation).

tween γ and the finite-difference approximation derived from the observed data during the period from sol 230 to sol 430 suggests that, at least during this period, the meridional structure of the tide is not strongly dependent on longitude.

4. Discussion

The theoretical interpretation of the tidal results has been given by Zurek (1981), but two aspects will be discussed here: the comparison of dust storm activity in the two years, and the probable significance of the dropout in the diurnal tide at the onset of 1977b.

Regardless of specific mechanism, the global dust storms are believed to require a buildup of dust load globally or regionally with the consequent increased heating and increased thermal forcing of winds (Gierasch, 1974; Leovy, 1979; Pollack *et al.*, 1979). Thus, the question of the mechanism for dust buildup prior to the onset of these storms is a key to understanding their initiation mechanism. The data show that in two years one global dust storm repeats very precisely with onset near $L_s = 200$, and one event fails to repeat. This suggests at least the possibility of two distinct mechanisms for generating the precursor dust: one closely locked to season, and the other one not. Briggs *et al.* (1979) and Peterfreund and Kieffer (1979) have shown that in 1977 there were two favored regions for local dust storms, the baroclinic zone adjacent to the edge of the retreating and subliming south polar cap, which had local dust storms before both global storms, and the elevated terrain near 20°S latitude, which had local storms prior to the second global storm. Even without baroclinic eddies, surface winds near the south polar cap edge can be expected to reach speeds approaching those required to raise dust (Leovy *et al.*, 1973; Haberle *et al.*, 1979; Haberle, 1979). Since the cap retreat follows a similar, though not identical, pattern each year, the frequency and intensity of these storms should be closely tied to the season. It is therefore reasonable to suppose that the 1977a and 1979a events arose in response to the precursor dust load and heating caused by these storms along the south polar cap edge. The 1979a event appears to have been weaker, possibly because the local storms were less intense or less frequent, or because the global-scale circulation during the period of these storms was less capable of spreading the dust vertically or horizontally over the planet.

The results of Ryan and Sharman (1981) and Barnes (1980, 1981) suggest another possible mechanism for precursor storms. Traveling waves in the Northern Hemisphere baroclinic zone begin to be active shortly before $L_s = 200$. These storms, whose onset is closely tied to the Northern Hemisphere baroclinicity, are known to raise dust also (Briggs and Leovy, 1974), and may contribute to general

Unauthenticated | Downloaded 03/03/24 03:50 PM UTC

dustiness in northern latitudes. The baroclinicity on which they depend is also closely locked to season. Thus either one, or perhaps both, of the baroclinic zones may contribute to the required dust loading. However, the dynamics of the two regions are probably very different since there are surface easterlies in the southern region, and surface westerlies in the north (Haberle *et al.*, 1979).

The 1977b event was preceded by numerous local storms in the uplands near 20°S. These storms and the diurnal tidal dropout prior to 1977b may be causally related to the onset of 1977b. The significance of the dropout comes into sharper focus in the light of classical tidal theory. Zurek's (1981) model yields a pressure amplitude for the Lander 1 diurnal tide that is within 20% of the observed tide over the entire period from sol 200 to sol 400 except for the dropout period when the observed and calculated tides differ by a factor of 5. The dropout suggests interference between the classical tidal modes and a mode not included in classical tidal theory. A likely candidate is the eastward-traveling diurnal Kelvin mode of wavenumber 1 ($S_1^{1,-1}$). It could interfere with the westward-traveling tide in the lowland longitudes of the Viking landers and reinforce the westward-traveling tide in tropical uplands, especially if the predominant forcing of this mode is the differential heating over uplands and lowlands. It is also near resonance in the Martian atmosphere, and is therefore sensitive to atmospheric thermal structure and heating distribution (Zurek, 1976). Selective excitation of this tidal component is therefore a candidate for explaining the occurrence of the precursor dust storms in the tropical southern uplands, the dropout in the diurnal tide at the onset of 1977b, and the initiation of global dust storms in some years but not in others.

Pressure observations from Lander 1 in future years and elaboration of the theory of topographically forced tides may permit validation or rejection of these proposed mechanisms.

APPENDIX

Details of the Semidiurnal Wind Model

The complex amplitudes of the eastward and northward components of the westward-propagating semidiurnal tide (u and v) are given, as in LZ, by

$$\left.\begin{aligned} i\sigma u - fv &= -isR\bar{T}(a\cos\phi)^{-1}P + Ku_{zz} \\ i\sigma v + fu &= -R\bar{T}a^{-1}P_{\phi} + Kv_{zz} \end{aligned}\right\}, \quad \text{(A1)}$$

where σ is the tidal frequency, R the gas constant, $\bar{T}$ the mean temperature, ϕ latitude, $P \equiv \delta p/\bar{p}$, and the subscripts indicate partial differentiation with respect to ϕ and height z. For the westward-traveling semidiurnal tide, $s = 2$, and $\sigma = fr/\sin\phi$ where $r = 0.998$ is the ratio of the sidereal to the solar day. These equations are solved, as in LZ, with the boundary conditions

$$(u,v) \to (u_s,v_s) \quad \text{as} \quad z \to \infty, \quad \text{(A2)}$$

$$Ku_z = \omega_0 u, \quad Kv_z = \omega_0 v \quad \text{at} \quad z = z_m, \quad \text{(A3)}$$

where (u_s,v_s) is the interior solution given in LZ.

The solution for constant K evaluated at z_m is

$$\left.\begin{aligned} u(z_m) &= Au_s - Bv_s \\ v(z_m) &= Av_s + Bu_s \end{aligned}\right\}, \quad \text{(A4)}$$

where

$$\left.\begin{aligned} A &= \{1 - [(1+\alpha_1) - i\alpha_1]/D_1 \\ &\qquad - [(1+\alpha_2) - i\alpha_2]/D_2\} \\ B &= \{[\alpha_1 + i(1+\alpha_1)]/D_1 \\ &\qquad - [\alpha_2 + i(1+\alpha_2)]/D_2\} \\ \alpha_1 &= (1+\sigma/f)^{1/2}\beta, \quad \alpha_2 = (\sigma/f - 1)^{1/2}\beta \\ D_i &= 2[1 + 2\alpha_i(1+\alpha_i)], \quad i = 1, 2 \end{aligned}\right\}. \quad \text{(A5)}$$

Observed values of P were used to evaluate these solutions, and for each case, values of γ (on which u_s and v_s depend) and β were found which minimized the rms residuals between the solutions and the observed $u(z_m)$, $v(z_m)$, with the complex values expressed as coefficients of the sine and cosine coefficients of the harmonic. The geostrophic drag coefficient C_g and the cross-isobar inflow angle were then determined by reevaluating A and B for the deduced value of β, but with $\sigma = 0$. Then

$$\left.\begin{aligned} C_g &= (A^2 + B^2), \quad \sigma = 0 \\ \theta &= \tan^{-1}(B/A), \quad \sigma = 0 \end{aligned}\right\}. \quad \text{(A6)}$$

Acknowledgments. I am grateful to Jeff Barnes and James Tillman for assistance with handling of the voluminous Viking data, and to Richard Zurek and Jack Ryan for making available copies of their papers in advance of publication. This research was supported by the Atmospheric Division of the Planetary Programs Office of NASA.

REFERENCES

Barnes, J. R., 1980: Time spectral analysis of mid-latitude disturbances in the Martian atmosphere. *J. Atmos. Sci.*, **34**, 2002–2015.

——, 1981: Mid-latitude disturbances in the Martian atmosphere: Second Mars year. *J. Atmos. Sci.*, **35** (in press).

Briggs, G. A., and C. Leovy, 1974: Mariner 9 observations of Mars' north polar hood. *Bull. Amer. Meteor. Soc.*, **55**, 278–296.

——, W. A. Baum and J. R. Barnes, 1979: Viking orbiter imaging observations of dust in the Martian atmosphere. *J. Geophys. Res.*, **84**, 2795–2820.

Unauthenticated | Downloaded 03/03/24 03:50 PM UTC

Gierasch, P. J., 1974: Martian dust storms. *Rev. Geophys. Space Phys.*, **12,** 730–734.

Haberle, R. M., 1979: The influence of Martian polar cap winds on the diurnal tide. *Icarus*, **39,** 184–191.

——, C. B. Leovy and J. B. Pollack, 1979: A numerical model of the Martian polar cap winds. *Icarus*, **39,** 151–183.

Hess, S. L., R. M. Henry, C. B. Leovy, J. A. Ryan and J. E. Tillman, 1977: Meteorological results from the surface of Mars: Viking 1 and 2. *J. Geophys. Res.*, **82,** 4559–4574.

Leovy, C. B., 1979: Martian meteorology. *Annual Review of Astronomy and Astrophysics*, Vol. 17, Annual Reviews, Inc., 387–413.

——, and R. W. Zurek, 1979: Thermal tides and Martian dust storms: direct evidence for coupling. *J. Geophys. Res.*, **84,** 2956–2968.

——, R. W. Zurek and J. B. Pollack, 1973: Mechanisms for Mars dust storms. *J. Atmos. Sci.*, **30,** 749–762.

Martin, T. Z., and H. H. Kieffer, 1979: Thermal infrared properties of the Martian atmosphere 2. The 15-μm band measurements. *J. Geophys. Res.*, **84,** 2843–2852.

Peterfreund, A. R., and H. H. Kieffer, 1979: Thermal infrared properties of the Martian atmosphere 3. Local dust clouds. *J. Geophys. Res.*, **84,** 2853–2863.

Pollack, J. B., D. S. Colburn, F. M. Flasar, R. Kahn, C. E. Carlston and D. Pidek, 1979: Properties and effects of dust particles suspended in the Martian atmosphere. *J. Geophys. Res.*, **84,** 2929–2945.

Ryan, J. A. and R. M. Henry, 1979: Mars atmospheric phenomena during major dust storms as measured at the surface. *J. Geophys. Res.*, **84,** 2821–2829.

——, and R. D. Sharman, 1981: Two major dust storms, one year apart: comparison from Viking data. *J. Geophys. Res.*, **86,** (in press).

Zurek, R. W., 1976: Diurnal tide in the Martian atmosphere. *J. Atmos. Sci.*, **33,** 321–337.

——, 1978: Solar heating of the dusty Martian atmosphere. *Icarus*, **35,** 196–208.

——, 1981: Inference of dust opacities for the 1977 Martian great dust storms from Viking Lander 1 pressure data. *Icarus,* **38** (in press).

Unauthenticated | Downloaded 03/03/24 03:50 PM UTC